INTERNATIONAL JOURNAL FOR NUMERICAL AND ANALYTICAL METHODS IN GEOMECHANICS
Int. J. Numer. Anal. Meth. Geomech., 2000; **24**:265–279

Pressure-dependent elastic moduli of granular assemblies

Ching L. Liao[1], Tian C. Chan[2], Akke S. J. Suiker[3]*† and Ching S. Chang[4]

[1] *Bureau of High Speed Rail, Taipei, Taiwan, R.O.C.*
[2] *China College of Industrial and Commercial Management, Taipei, Taiwan, R.O.C.*
[3] *Koiter Institute Delft/Faculty of Civil Engineering, Delft University of Technology, P.O. Box 5048, 2600 GA Delft, The Netherlands*
[4] *Department of Civil and Environmental Engineering, University of Massachusetts, Amherst, MA 01003, U.S.A.*

SUMMARY

Conventional homogenization theories developed for a matrix-inclusion system cannot be used for deriving the pressure-dependent elastic behaviour of a granular material. This is caused by the lack of a proper description of the high stress concentrations at the particle contacts. This paper discusses a more suitable homogenization theory, which follows from micro-structural considerations at the particle level. Accordingly, for an assembly of isotropically distributed, equal-sized spherical particles, expressions for the pressure-dependent shear modulus and the Poisson's ratio are derived. This is done for the case of hydrostatic compression. The derivation of these equations is based on the so-called *best-fit hypothesis* of the actual displacement field in the granular assembly. The usefulness of the equation derived for the shear modulus is illustrated via a comparison with experiment results. Copyright © 2000 John Wiley & Sons, Ltd.

KEY WORDS: pressure-dependent elasticity; micromechanics; homogenisation

1. INTRODUCTION

In general, granular materials such as sand and gravel can be considered as an assembly of discrete particles. When applying a confining pressure on the assembly, it behaves as a continuous solid because the individual particles are then prevented from segregation. The elastic stiffness properties of the granular continuum depend on the magnitude of the confining pressure, since an increasing (*decreasing*) confining pressure increases (*decreases*) the contact area between the particles, which causes an increase (*decrease*) of the inter-particle contact stiffness. By identifying the granular assembly as a two-phase material, where the particles correspond to the solid phase and the voids correspond to the gas phase, it can thus be stated that the solid phase determines the overall stiffness behaviour in a non-linear manner.

The stiffness properties of a granular assembly can be related to the stiffness properties of the granular micro-structure by using homogenization theories. Traditionally, homogenization theories for two-phase materials have been widely applied for matrix-inclusion systems, such as composites and porous rocks. In this paper, we will start with evaluating the applicability of

* Correspondence to: A. S. J. Suiker, Delft University of Technology, Faculty of Civil Engineering, P.O. Box 5048, 2600 GA Delft, The Netherlands
† E-mail: A.Suiker@ct.tudelft.nl

Received 1 March 1999
Revised 11 June 1999

several of these homogenization methods to granular materials. This will be done by comparing their shear modulus prediction with that of experimental results. It will be shown that for granular materials these homogenization methods lead to an overestimation of the shear stiffness, which is caused by the lack of a proper capturing of the high stress concentrations at the particle contacts.

Homogenization theories more suitable for granular materials start with considering the pressure-dependent elastic behaviour of two spheres at direct contact. Accordingly, a non-linear elastic contact law according to the Hertz theory[1–3] may be incorporated, which has been done for regular packings by Duffy and Mindlin[4] and Deresiewicz[5] as well as for irregular packings by Digby,[6] Walton[7] and Chang *et al.*[8] However, these homogenization theories are all based on the so-called *kinematic hypothesis* (or Voigt's hypothesis), which states that every particle within the assembly displaces in accordance with a uniform deformation field. This assumption actually implies a constraint on the granular assembly, resulting in an *overestimation* of the true pressure-dependent stiffness behaviour in the assembly. The use of a kinematic hypothesis can be circumvented by trying to find a more realistic relation for the displacement field in the assembly. In a previous paper,[9] this has been done by postulating that the mean displacement field in the assembly is the best fit of the actual displacement field. This hypothesis has been named the *best-fit hypothesis*, which relaxes the constraint that is used in the kinematic hypothesis. Using the best-fit hypothesis, two micro–macro relationships can be derived, namely the contact displacement-to-strain relationship and the contact force-to-stress relationship. Together with the Hertzian contact law, the complete homogenization framework is then defined. By back-fitting the results of shear stiffness measurements on round-grained Ottawa sand, it will be demonstrated that the homogenization procedure that relies on the best-fit hypothesis leads to an *underestimation* of the true pressure-dependent stiffness behaviour. If this result is combined with that by the kinematic hypothesis which leads to an overestimation, a useful range for the true pressure-dependent elastic behaviour can be found.

2. HOMOGENIZATION METHODS FOR A TWO-PHASE MATERIAL

For a two-phase material, the *relative shear stiffness* may be defined as the ratio between the effective shear modulus of the total assembly G_{eff} and the shear modulus of the solid phase G. The effective shear modulus can be experimentally determined by measuring the shear wave velocity under a low-strain cycle torsial deformation ($\varepsilon_{\text{tor}} < 0{\cdot}01$ per cent) that is applied on a cylindrical specimen. Such experiments reveal that for an assembly of discrete particles, such as glass beads[10] or sands,[11,12] the range of the relative shear stiffness is 10–60 times lower than that of porous media, such as sintered glass beads[13] or porous rock.[14] This is illustrated in Figure 1, showing the variation of the relative shear stiffness versus the void ratio of the specimen, where the confining pressure varies between 10 and 80 psi (= 69 and 552 kPa). Also, the predictions by several homogenization methods have been depicted, to which we will return later. Since for the tests in Figure 1 the applied strain level is relatively small and the confining pressure is relatively high, it is unlikely that permanent inter-particle slip occurs, so that it may be expected that the particle contacts behave mainly reversible. The reason for the low relative shear stiffness of the granular material is that the individual particles transmit the overall deformation via concentrated contact points, which results in *high stress concentrations* and thus in a low assembly stiffness.

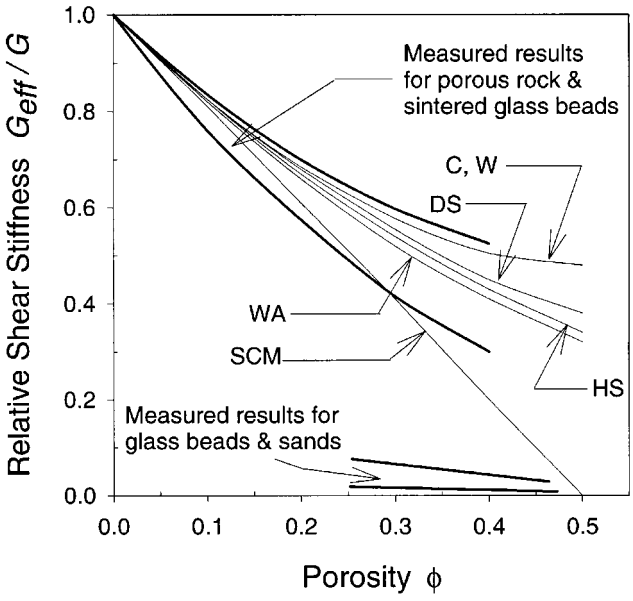

Figure 1. The relative shear stiffness versus the porosity for various materials; measurements and predictions by homogenization methods

Traditional homogenization theories that were developed for matrix-inclusion systems contemplate the so-called dilute dispersion of the inclusions,[15,16] which means that the fractional concentration of the inclusions is much lower than the fractional concentration of the matrix. Consequently, these theories cannot describe high stress concentrations at the inclusions, which makes them inappropriate for application to granular materials. More recently, theories have been developed for non-dilute matrix-inclusion systems, which better predict high stress concentrations at the inclusions. In this category we find the self-consistent scheme (= SCM) by Hill[17] and by Budiansky,[18] the differential scheme (= DS) by Zimmerman[19] and other theories by Walpole[20] (= W), Chatterjee *et al.*[21] (= C), Hashin–Shtrickman[22] (= HS) and Willis and Acton[23] (= WA). In Figure 1 the prediction by these methods has been plotted. Apparently, for the porous rock and sintered glass beads the predictions are good, but it is obvious that the stiffness behaviour of the glass beads and the sand is predicted poorly. This is caused by the fact that stress concentrations at particle contacts are much higher than in most non-dilute matrix-inclusion systems.

3. MICROMECHANICS OF A GRANULAR ASSEMBLY

A suitable homogenization technique regarding the pressure-dependent elastic behaviour of granular materials requires incorporation of the micro-mechanical behaviour of individual particles in direct contact. When modelling the individual particles as elastic spheres, Hertz theory[1] can be used for describing the non-linear particle interaction. This theory has been thoroughly discussed by many investigators,[24,2,25,3] and will be briefly reported here because it will be used later for deriving the elastic moduli for a particle assembly.

3.1. Elastic inter-particle contact behaviour

We start with considering two dissimilar particles with different Poisson's ratios v_1, v_2, Young's moduli E_1, E_2 and radii R_1, R_2. When the two spheres are compressed by a magnitude δ_n, which is the normal contact displacement, the relation with the resulting contact force f_n is given by[3]

$$\delta_n^3 = \frac{9f_n^2}{16M^2L} \tag{1}$$

where

$$\frac{1}{L} = \frac{1}{R_1} + \frac{1}{R_2}, \qquad \frac{1}{M} = \frac{1 - v_1^2}{E_1} + \frac{1 - v_2^2}{E_2} \tag{2}$$

In this study, it is assumed that the individual particles have identical characteristics, so that $R = R_1 = R_2$, $v = v_1 = v_2$, $L = R/2$ and $M = G/(1 - v)$.

Expression (1) is non-linear, which is caused by the stiffening effect under increasing particle movement. The increasing contact area under an increasing particle movement can be formulated as[3]

$$\delta_n = \frac{a^2}{L} \tag{3}$$

with a the radius of the circular contact. Combining equation (3) with equation (1), a measure for the contact area in terms of the contact force is obtained

$$a^3 = \frac{3Lf_n}{4M} \tag{4}$$

In order to determine an expression for the contact stiffness, expression (1) is rewritten into a force–displacement relation

$$f_n = \sqrt{\frac{16M^2L\delta_n^3}{9}} \tag{5}$$

from which we can straightforwardly derive the normal contact stiffness as

$$K_n = \frac{\partial f_n}{\partial \delta_n} = 2M\sqrt{L\delta_n} = 2Ma \tag{6}$$

thereby using equation (3). When combining equation (4) with equation (6), the normal contact stiffness in terms of the contact force becomes

$$K_n = (6L)^{1/3}M^{2/3}f_n^{1/3} \tag{7}$$

which relation will be used later for deriving the pressure-dependent elastic moduli of a granular assembly. Assuming an *ideal elastic contact situation*, the transversal contact stiffness may be expressed in terms of the normal contact stiffness via

$$K_s = \alpha K_n \tag{8}$$

where α is related to the Poisson's ratio of the particles[2]

$$\alpha = \frac{2(1-\nu)}{2-\nu} \tag{9}$$

In the expressions above the contact between two circular particles is assumed to be ideally elastic, where both particles are considered to behave like an elastic half-space that is loaded by a parabolic contact pressure distribution.[2] However, in natural sands the particles are normally rough, where at the contact they do not behave like ideal elastic half-spaces. Also, the particles may undergo plastic deformations. By analysing the experimental data for sands and rocks, several investigators have therefore proposed to slightly modify equations (7)–(9) in order to incorporate such effects. For example, for sands the exponent for the normal contact force in equation (7) is often chosen between one fourth and one-half,[26] and also equation (8) is often extended with a term that governs frictional sliding of particles,[8] i.e.

$$K_s = \alpha K_n \left(1 - \frac{f_s}{f_n \tan \varphi_u}\right)^{\eta} \tag{10}$$

with f_s the transversal contact force, φ_u the friction angle at the particle contact surface and η a fitting parameter. Apparently, equation (10) causes that the ratio between the transversal contact stiffness and normal contact stiffness is not constant anymore, but depends on the magnitude of the contact shear force f_s. Although the framework that will be presented in this paper can incorporate such a modification, we will limit ourselves to isotropic granular assemblies under hydrostatic compression, for which $f_s = 0$. Equation (10) then reduces to the elastic contact condition given by equations (8) and (9).

3.2. *Micro–macro relationships*

In the 1950's the non-linear contact behaviour according to Hertz theory was applied for homogenisation of regular packings of equal-sized spheres.[4,5] More recently, homogenization procedures were proposed for randomly packed, equal-sized spheres.[6–8] All these studies are based on a *kinematic hypothesis*, stating that every particle within the assembly displaces in accordance with a uniform deformation field, i.e.

$$\delta_i^c = \varepsilon_{ij} L_j^c \tag{11}$$

where δ_i^c is the displacement between two particle centres, known as the contact displacement, where the superscript 'c' denotes 'contact'. Furthermore, ε_{ij} is the overall assembly strain and L_j^c the branch vector, which is the distance between the centres of two particles in contact. As mentioned in the introduction, the kinematic hypothesis (11) imposes a constraint on the granular assembly, making it necessary that the formulation governs a response that is stiffer than the true behaviour. Together with this kinematic relation, a second micro–macro relation needs to be formulated, which couples the inter-particle contact forces to the assembly stress. In the field of micro–macro mechanics this formulation follows from the theorem of mean stress, or from the principle of virtual work,[27,6–8] yielding

$$\sigma_{ij} = \frac{1}{V} \sum_{c=1}^{N} f_j^c L_i^c \tag{12}$$

where σ_{ij} is the average stress in the assembly, V the volume of the assembly, f_j^c is the inter-particle contact force at the contact and N the total number of contacts in the assembly.

In this paper, we aim to derive the pressure-dependent stiffness moduli using a *best-fit hypothesis*, instead of the kinematic hypothesis, as the best-fit hypothesis circumvents the constraint by equation (11). This hypothesis has been proposed in a previous paper,[9] in which by comparison with a discrete element model for a linear elastic granular material it has been demonstrated that this method leads to an *underestimation* of the true stiffness behaviour. The softer behaviour is caused by the fact that the best-fit hypothesis considers a mean displacement field to fit the true displacement field, where the kinematic compatibility between the individual particles is not necessarily required. Similar to equations (11) and (12), for the best-fit hypothesis also (1) a contact displacement-to-strain relationship and (2) a contact force-to-stress relationship can be established.

Contact displacement-to-strain relationship

As pointed out in Liao *et al.*,[9] for the derivation of the displacement-to-strain relationship the actual contact displacement field δ_i^c in the assembly is considered to fluctuate about the mean displacement field $\varepsilon_{ij}L_j^c$. The difference between both displacement fields can then be defined as

$$E_i = \delta_i^c - \varepsilon_{ij}L_j^c \tag{13}$$

In correspondence with a least-squares method, a measure for the difference over the total number of contacts can be written in a scalar format S as

$$S = \sum_{c=1}^{N} (\delta_i^c - \varepsilon_{ij}L_j^c)^2 \tag{14}$$

By postulating that the mean displacement field is the best fit for the actual displacement field, the mean displacement field can be derived via minimizing S with respect to the assembly strain ε_{mn}

$$\frac{\partial S}{\partial \varepsilon_{mn}} = 0 \tag{15}$$

which leads to

$$\sum_{c=1}^{N} (\delta_i^c - \varepsilon_{ij}L_j^c) \frac{\partial}{\partial \varepsilon_{mn}} (\delta_i^c - \varepsilon_{ij}L_j^c) = 0 \tag{16}$$

Expression (16) can be further elaborated as

$$\sum_{c=1}^{N} (\varepsilon_{mj}L_j^c L_n^c - \delta_m^c L_n^c) = 0 \tag{17}$$

where, since ε_{ij} is the average strain over the assembly, this equation may also be written as

$$\varepsilon_{mj}V \sum_{c=1}^{N} \frac{1}{V} L_j^c L_n^c = \sum_{c=1}^{N} \delta_m^c L_n^c \tag{18}$$

finally yielding

$$\varepsilon_{ij} = \frac{1}{V} \sum_{c=1}^{N} \delta_i^c L_n^c A_{jn} \tag{19}$$

with A_{jn} the fabric tensor

$$A_{jn} = \left[\frac{1}{V} \sum_{c=1}^{N} L_j^c L_n^c \right]^{-1} \tag{20}$$

It can be noted that the character of expression (19) is considerably different from the displacement-to-strain relationship according to the kinematic hypothesis (equation (11)).

For a granular assembly that consists of equal-sized spherical particles with an isotropic distribution of inter-particle contacts, the summation over a contact quantity F^c may be replaced by an integral form

$$\sum_{c=1}^{N} F^c(\gamma, \beta) = \frac{N}{4\pi} \int_0^{2\pi} \int_0^{\pi} F^c(\gamma, \beta) \sin \gamma \, \mathrm{d}\gamma \, \mathrm{d}\beta \tag{21}$$

where γ is the angle of declination and β the angle of rotation in a spherical co-ordinate system. Using the fact that the branch vector then equals $L_i^c = 2Rn_i^c$, with n_i^c is the basic unit vector in the direction normal to the particle contact, the fabric tensor in equation (20) can be expressed as

$$A_{jn} = \left[\frac{4R^2 N}{3V} \delta_{jn} \right]^{-1} \tag{22}$$

where δ_{jn} is the well-known Kronecker delta symbol.

Contact force-to-stress relationship

Apart from the relation between the assembly strain and the contact displacements, a relation between the assembly stress and the contact forces needs to be determined. This can be done via the principle of energy conservation.[28,29,9] The incremental complimentary work ΔW for an assembly with volume V, as commonly evaluated via the global stress σ_{ij} and the global incremental strain $\Delta\varepsilon_{ij}$, may also be evaluated via the contact forces f_i^c and the incremental contact displacements $\Delta\delta_i^c$, yielding

$$\Delta W = V \sigma_{ij} \Delta \varepsilon_{ij} = \sum_{c=1}^{N} f_i^c \Delta \delta_i^c \tag{23}$$

where N is the total number of contacts in the particle assembly. When substituting an incremental form of equation (19) into equation (23), the following relationship between the contact force f_i^c and the average stress σ_{ij} can be derived

$$f_i^c = \sigma_{ij} L_n^c A_{jn} \tag{24}$$

which obviously differs from the stress-to-contact force relationship, equation (12), corresponding to the kinematic hypothesis. The format of equation (24) has also been reported by other authors,[28,29] although in their work this so-called 'static equation' was introduced via heuristic reasoning. For an isotropic packing structure, substitution of the isotropic fabric tensor, equation (22) into equation (24) relates the contact force f_i^c for a given direction n_j^c *directly* to the assembly stress σ_{ij}

$$f_i^c = \frac{3V}{2RN} \sigma_{ij} n_j^c \tag{25}$$

where the ratio N/V governs the density of the assembly. Instead of using N/V for denoting the density, it is more common to use the co-ordination number and the porosity. The co-ordination number $\bar{n}$ is defined by

$$\bar{n} = \frac{2N}{N_p} \tag{26}$$

where N_p is the total number of particles in the assembly. In equation (26) the factor 2 appears because two particles generate one contact. Additionally, the porosity ϕ of the assembly reads

$$\phi = \frac{V_v}{V} \tag{27}$$

in which V_v is the total volume of the voids. For equal-sized spherical particles the total particle volume V_p follows from

$$V_p = N_p \tfrac{4}{3}\pi R^3 \tag{28}$$

where R is the particle radius. By using the fact that $V = V_p + V_v$, a combination of equations (26)–(28) leads to

$$\frac{N}{V} = \frac{3}{8}\frac{\bar{n}(1-\phi)}{\pi R^3} \tag{29}$$

where, for reasons of convenience, equation (29) will be expressed as

$$\frac{N}{V} = \frac{3}{2R^3\theta} \tag{30}$$

with θ the packing parameter

$$\theta = \frac{4\pi}{(1-\phi)\bar{n}} \tag{31}$$

Substituting equation (30) into equation (25) we obtain for the contact force

$$f_i^c = \theta R^2 \sigma_{ij} n_j^c \tag{32}$$

For a randomly packed assembly of particles, the relationship between the co-ordination number $\bar{n}$ and the porosity ϕ is not unique. On the other hand, for regular packings this relationship can be determined precisely,[30] and has been depicted in Figure 2 for a simple cubic packing ($\bar{n} = 6$, $\phi = 0{\cdot}4764$), a tetragonal sphenoidal packing ($\bar{n} = 8$, $\phi = 0{\cdot}3954$), a pyramidal packing ($\bar{n} = 10$, $\phi = 0{\cdot}3019$), and a tetrahedral packing ($\bar{n} = 12$, $\phi = 0{\cdot}2595$). It can be expected that for a random packing the relation between the co-ordination number and the porosity will not deviate much from the trend in Figure 2.

Instead of using the relation in Figure 2, we can also apply an experimentally determined relation between the co-ordination number and the porosity, for example, such as the one proposed by Yanagisawa (1983) for gravels with round and flat shapes. The current framework is certainly flexible for such adaptations.

3.3. Non-uniform stress at particle contacts

For demonstrating that the stress non-uniformity is captured by the current model, we will consider the ratio between the (local) contact stress and the (global) assembly stress, where the

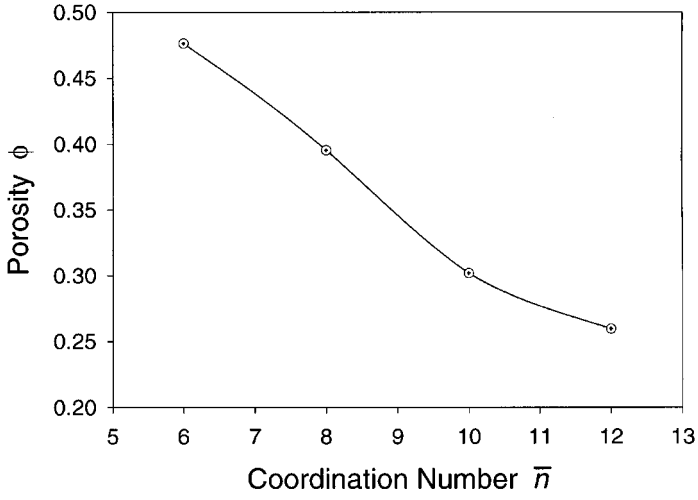

Figure 2. Relationship between porosity ϕ and co-ordination number $\bar{n}$

contact stress σ_n reads

$$\sigma_n = \frac{f_n^c}{\pi a^2} \tag{33}$$

where a is the radius of the circular contact area. By considering a state of hydrostatic compression, i.e. $\sigma_{ij} = \sigma_0 \delta_{ij}$, the contact force equation (32) becomes

$$f_n^c = \theta R^2 \sigma_0 \tag{34}$$

Combining equations (34), (31) and (33), we obtain

$$\frac{\sigma_n}{\sigma_0} = \frac{4}{(1-\phi)\bar{n}} \left(\frac{R}{a}\right)^2 \tag{35}$$

In correspondence with equation (35), in Figure 3 we have plotted the confining pressure σ_0 versus the contact stress σ_n for the regular packings that have been discussed in Section 3.2. For simplicity, we have thereby assumed that the grain radius R equals the radius of the contact area a. It can be noted that for a higher density (= increasing co-ordination number $\bar{n}$), the contact pressure decreases, which is the result of an increasing number of contact points.

Equation (35) can also be used for depicting the relation between the normalized contact radius a/R versus the relative contact pressure σ_n/σ_0 (Figure 4). Apparently, when the ratio between the contact area radius and the particle radius decreases, the contact becomes more local, resulting in a higher contact stress. For sufficiently small contact areas, i.e., a/R goes to zero, the particle contact will not behave elastic anymore since particle crushing then occurs. Although this effect may be incorporated by defining an elastic threshold with respect to the normal contact force f_n^c (which implies a maximum value for the normal contact stiffness K_n in equation (7)), the stress levels that will be considered in this study will remain under the threshold of particle crushing.

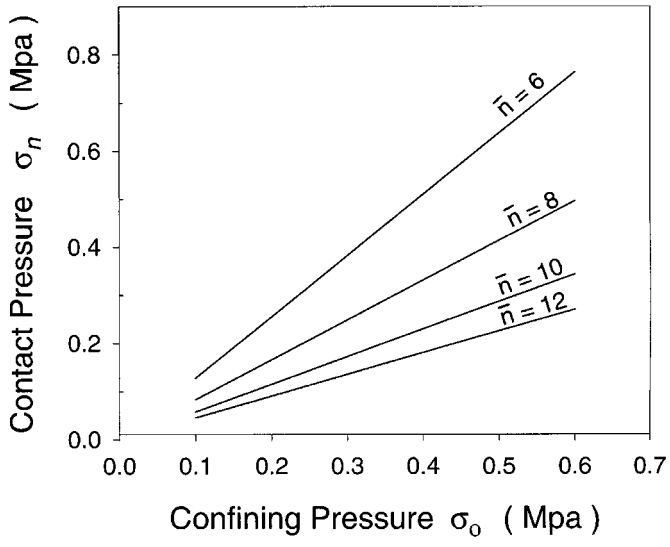

Figure 3. Contact pressure σ_n versus confining pressure σ_0 for different packings $\bar{n}$

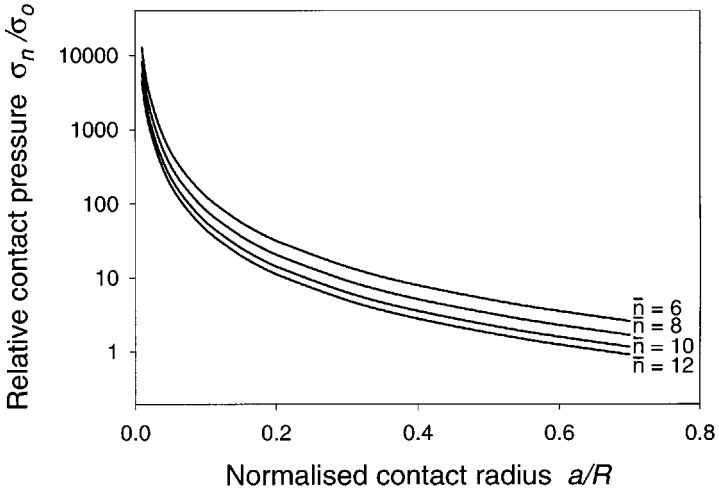

Figure 4. The relative contact pressure σ_n/σ_0 versus the normalized contact radius a/R for different packings $\bar{n}$

4. STRESS–STRAIN RELATIONSHIP

In order to derive the pressure-dependent stiffness moduli in an isotropic granular assembly, we start with formulating the stress–strain flexibility relation

$$\varepsilon_{ij} = H_{ijkl}\sigma_{kl} \tag{36}$$

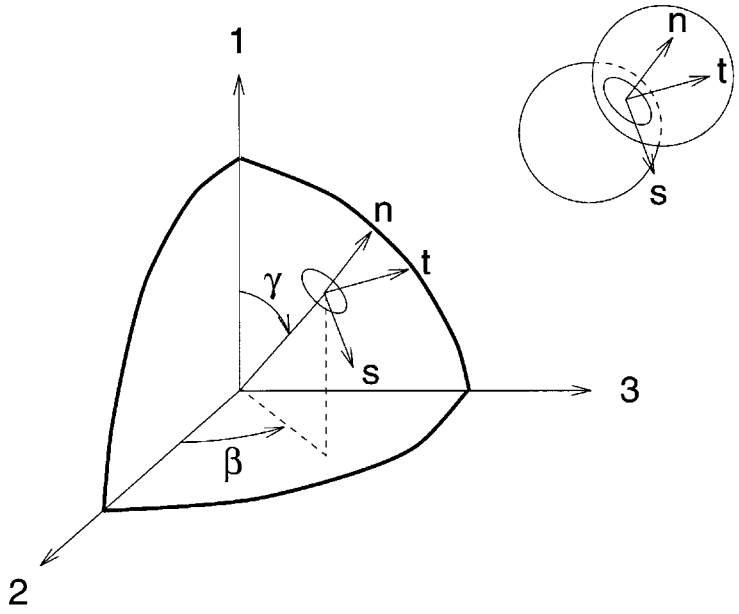

Figure 5. Local and global co-ordinate system at the particle contact

where H_{ijkl} represents the macroscopic flexibility tensor. The macroscopic flexibility tensor depends on the flexibility S_{ij}^c on a particle level, which parameter relates the inter-particle force f_j^c to the inter-particle displacement δ_i^c

$$\delta_i^c = S_{ij}^c f_j^c \tag{37}$$

The flexibility tensor S_{ij}^c can be expressed in terms of the normal contact stiffness K_n and the tangential contact stiffness K_s and K_t between two particles

$$S_{ij}^c = \frac{1}{K_n} n_i^c n_j^c + \frac{1}{K_s} s_i^c s_j^c + \frac{1}{K_t} t_i^c t_j^c \tag{38}$$

where $\mathbf{n}^c$, $\mathbf{s}^c$ and $\mathbf{t}^c$ are the basic unit vectors of the local co-ordinate system constructed at a particle contact (Figure 5). The vector $\mathbf{n}^c$ is directed normal to the contact plane and the vectors $\mathbf{s}^c$ and $\mathbf{t}^c$ are directed transversal to the contact plane, which can be formulated as

$$\begin{aligned} \mathbf{n}^c &= (\cos\gamma, \sin\gamma\cos\beta, \sin\gamma\sin\beta) \\ \mathbf{s}^c &= (-\sin\gamma, \cos\gamma\cos\beta, \cos\gamma\sin\beta) \\ \mathbf{t}^c &= (0, -\sin\beta, \cos\beta) \end{aligned} \tag{39}$$

where γ and β are the angles in the spherical co-ordinate system (Figure 5). An explicit expression for the overall flexibility tensor H_{ijkl} can now be obtained by combining (19), (22), (24), (30), (36) and (37), yielding

$$H_{ijkl} = \frac{3\theta R}{2N} \sum_{c=1}^{N} S_{ik}^c n_j^c n_L^c \tag{40}$$

For a representative volume with a large number of contacts that are isotropically distributed, equation (40) can be replaced by an integral form as pointed out in equation (21). This leads to

$$H_{ijkl} = \frac{3\theta R}{8\pi} \int_0^{2\pi} \int_0^{\pi} S_{ik}^c(\gamma, \beta) n_j^c(\gamma, \beta) n_l^c(\gamma, \beta) \sin\gamma \, \mathrm{d}\gamma \, \mathrm{d}\beta \tag{41}$$

Carrying out this integration, for an ideal isotropic granular structure ($K_s = K_t$), the effective shear modulus G_{eff} and the effective Poisson's ratio v_{eff} follow the expressions

$$G_{\text{eff}} = \frac{5K_n}{R\theta}\left(\frac{\alpha}{3+2\alpha}\right)$$

$$v_{\text{eff}} = \frac{1-\alpha}{2+3\alpha} \tag{42}$$

with $\alpha = K_s/K_n$, in agreement with equation (8). An expression for the pressure-dependent elastic moduli can then be obtained by combining (7), (31), (34) and (42), which yields

$$\frac{G_{\text{eff}}}{G} = \frac{5\alpha}{3+2\alpha}\left(\frac{\sqrt{3}\bar{n}(1-\phi)}{4\pi(1-v)}\right)^{2/3}\left(\frac{\sigma_0}{G}\right)^{1/3} \tag{43a}$$

$$v_{\text{eff}} = \frac{1-\alpha}{2+3\alpha} \tag{43b}$$

It is interesting to compare equation (43) as derived via applying the best-fit hypothesis with the elastic moduli that follow from applying the kinematic hypothesis[8]

$$\frac{G_{\text{eff}}}{G} = \frac{2+3\alpha}{5}\left(\frac{\sqrt{3}\bar{n}(1-\phi)}{4\pi(1-v)}\right)^{2/3}\left(\frac{\sigma_0}{G}\right)^{1/3} \tag{44a}$$

$$v_{\text{eff}} = \frac{1-\alpha}{4+\alpha} \tag{44b}$$

Except for the first term, the expressions for the effective shear modulus (43a) and (44a) have a surprisingly similar character, while the effective Poisson's ratio (43b) and (44b) are very different. The shear modulus (*Poisson's ratio*) obtained via the best-fit hypothesis is smaller (*larger*) than that obtained via the kinematic hypothesis. The best-fit hypothesis thereby provides an underestimation while the kinematic hypothesis provides an overestimation of the true stiffness behaviour. Accordingly, the two expressions may present a range that captures the shear modulus as obtained from experiments. This can be demonstrated by depicting equations (43a) and (44a) together with the shear modulus measurements for 'round grained' Ottawa sand[26] at various porosity ϕ (Figure 6). The experimental results were obtained for a confining pressure of 41·62 psi (0·287 MPa). The model predictions in Figure 6 correspond to a back-calculated shear modulus for the sand particles of $G = 20{,}963$ MPa, and a Poisson's ratio of $v = 0{\cdot}15$, which are realistic values for sand particles. The value for α has been determined via equation (9), while the coordination number $\bar{n}$ follows from its dependency on the porosity ϕ (Figure 2). As Figure 6 illustrates, the predictions capture the magnitude as well as the trend of the measurements quite well.

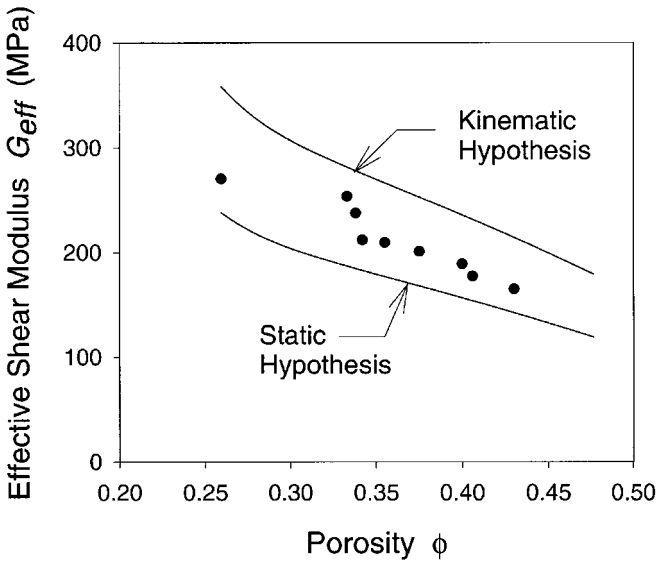

Figure 6. Effective shear modulus G_{eff} versus the porosity; predictions (lines) and measurements (dots) for 'round grained' Ottawa sand[26]

5. CONCLUSIONS

Conventional homogenization theories developed for matrix-inclusion systems do not give accurate predictions for the elastic behaviour of granular materials, which is caused by the lack of a proper description of the high stress concentrations at the particle contacts. As a result, these homogenization theories predict an elastic stiffness that is 10–60 times higher than that measured from experiments on assemblies of discrete particles.

In this paper a more suitable homogenization theory for granular material has been presented, which is based on the mechanical behaviour at particle contact level. Expressions for the pressure-dependent elastic moduli have been derived using *best-fit hypothesis* in combination with a non-linear inter-particle contact law of the Hertzian type. While homogenization theories that use the kinematic hypothesis lead to an overestimation of the true stiffness behaviour, use of the best-fit hypothesis results in an underestimation. As demonstrated, both theories may provide a range that captures the measured stiffness response of a granular assembly.

Since it has been assumed that the granular material consists of spherical particles, for more angular sand particles the model presented by equation (43) may lead to less accurate predictions. Another factor for deviations may be that under relatively low confining pressures the particles in the assembly tend to slide, which behaviour is not captured by the current model. Regarding such aspects, it is emphasized that equation (43) is not meant to cover the pressure-dependent behaviour of any granular material under arbitrary stress conditions. The main purpose has been to demonstrate how the elastic stiffness of an assembly of randomly packed, equal-sized, spherical particles can be derived in a relatively simple manner from the inter-particle contact conditions, where different hypotheses are possible. Besides, it has been noted that within the current framework it is possible to include effects such as particle friction and angularity, via

modifications of the inter-particle stiffness in equations (7)–(9). However, the inclusion of particle friction (equation (10)), which becomes relevant when anisotropic effects start to play a role, causes that a closed-form solution as presented in equation (43) is difficult, if not impossible, to retrieve. Under such circumstances a numerical evaluation of the pressure-dependent behaviour is most likely required.

REFERENCES

1. H. Hertz, 'Über die Berührung fester elasticher Körper', *J. Reine U. Angew. Math*., **92,** 156–171 (1881).
2. R. D. Mindlin and H. Deresiewicz, 'Elastic spheres in contact under varying oblique forces', *ASME*, *J. Appl. Mech*., **20,** 327–344 (1953).
3. K. L. Johnson, *Contact Mechanics*, Cambridge University Press, London, England, 1985.
4. J. Duffy and R. D. Mindlin, 'Stress–strain relations and vibrations of a granular medium', *ASME*, *J. Appl. Mech*., **24,** 585–593 (1957).
5. H. Deresiewicz, 'Stress–strain relations for a simple model of a granular medium', *ASME*, *J. Appl. Mech*., **25,** 402–406 (1958).
6. P. J. Digby, 'The effective elastic moduli of porous granular rock', *ASME*, *J. Appl. Mech*., **48,** 803–808 (1981).
7. K. Walton, 'The effective elastic moduli of a random packing of spheres', *J. Mech. Phys. Solids*, **35,** 213–226 (1987).
8. C. S. Chang, S. S. Sundaram and A. Misra, 'Initial moduli of particulated mass with frictional contacts', *Int. J. Numer. Anal. Meth. Geomech*., **13,** 626–641 (1989).
9. C. L. Liao, T. P. Chang, D. H. Young and C. S. Chang, 'Stress–strain relationships for granular materials based on the hypothesis of best fit', *Int. J. Solids Structures*, **34,** 4087–4100 (1997).
10. E. Yanagisawa, 'Influence of void ratio and stress condition on the dynamic shear modulus of granular media', in J. T. Jenkins and M. Satake (eds), *Advances in the Mechanics and Flow of Granular Materials*, Elsevier, Amsterdam, 1983, pp. 947–960.
11. B. O. Hardin and V. P. Drnevich, 'Shear modulus and damping in soils: measurements and parameter effects', *ASCE*, *J. Soil Mech. Found. Div*., **92,** 603–624 (1972).
12. R. M. Chung, F. Y. Yokel and V. P. Drnevich, 'Evaluation of dynamic properties of sands by resonant column testing', *ASTM*, *Geotech. Test. J*., **7,** 60–69 (1984).
13. J. B. Walsh, W. F. Brace and A. W. England, 'Effect of porosity in compressibility of glass', *J. Amer. Ceramic Soc*., **48,** 605–608 (1965).
14. J. G. Berryman and P. A. Berge, 'Rock elastic properties: dependence on microstructure', *in* C. S. Chang and J. W. Ju (Eds) *Homogenization and Constitutive Modelling for Heterogeneous Materials*, AMD-Vol. 166, ASME, New York, pp. 1–97.
15. J. N. Dewey, 'The elastic constants of materials loaded with non-rigid fillers', *J. Appl. Phys.* **18,** 578–581 (1947).
16. J. D. Eshelby, 'The determination of elastic field of an ellipsoidal inclusion, and related problems', *Proc. Roy. Soc. London Ser. A*, **241,** 376–396 (1957).
17. R. Hill, 'A self-consistent mechanics of composite materials', *J. Mech. Phys. Solids*, **13,** 213–222 (1965).
18. B. Budiansky, 'On the elastic moduli of some heterogeneous materials', *J. Mech. Phys. Solids*, **13,** 223–227 (1965).
19. R. W. Zimmerman, 'Elastic moduli of solid with spherical pores: new self-consistent method', *Int. J. Rock Mech. Mining Sci. Geomech. Abstr*., **21,** 339–343 (1984).
20. L. J. Walpole, 'The elastic behavior of a suspension of spherical particles', *Q. J. Mech. Appl. Math*., **25,** 153–160 (1972).
21. A. K. Chatterjee, A. K. Mal and L. Knopoff, 'Elastic moduli of two component systems', *J. Geophys. Res*., **83,** 1785–1792 (1976).
22. Z. Hashin, and S. Shtrikman, 'On some variational principles in anisotropic and non-homogeneous elasticity', *J. Mech. Phys. Solids*, **10,** 335–342 (1962).
23. J. R. Willis, and J. R. Acton, 'The overall elastic moduli of a dilute suspension of spheres', *Quart. J. Mech. Appl. Math*., **29,** 163–177 (1976).
24. S. P. Timoshenko and J. N. Goodier, *Theory of Elasticity*', McGraw-Hill Book Co. New York, 1951.
25. K. Walton, 'The oblique compression of two elastic spheres', *J. Mech. Phys. Solids*, **26,** 139–150 (1978).
26. B. O. Hardin and F. E. Richart, 'Elastic wave velocities in granular soils', *ASCE*, *J. Soil Mech. Found. Div*., **89,** 33–65 (1963).

27. J. Christofferson, M. M. Mehrabadi and S. Nemat-Nassar, 'A micromechanical description on granular material behaviour', *ASME J. Appl. Mech.*, **48,** 339–344 (1981).
28. B. Cambou, P. Dubujet, F. Emeriault and F. Sidoroff, 'Homogenization for granular materials', *Eur. J. Mech. A/Solids*, **14,** 255–276 (1995).
29. C. S. Chang, and J. Gao, 'Kinematic and static hypothesis for constitutive modeling of granulates considering particle rotation', *Acta Mech.*, **115,** 213–229 (1996).
30. F. E. Richart, R. D. Woods and J. R. Hall, *Vibrations of Soils and Foundations*, Prentice-Hall, Englewood Cliffs, NJ, 1970.

